Figure S1

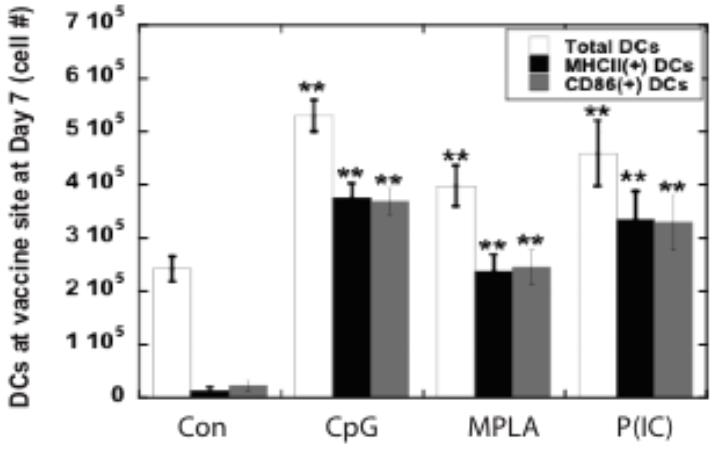

Figure S1 – **Activated dendritic cell numbers at the vaccine implant site**. The total numbers of CD11c(+) DCs, and CD11c(+) DCs positive for MHCII and CD86 expression, at the scaffold site at day 7 after implantation of GM-CSF loaded matrices (Con) and matrices loaded with GM-CSF in combination with CpG-ODN (CpG), MPLA (MPLA), and P(I:C) (P(IC)). Values represent mean and standard deviations (n=6). * $P<0.05$ ** $P<0.01$, as compared to GM-CSF loaded matrices (Con).

Figure S2

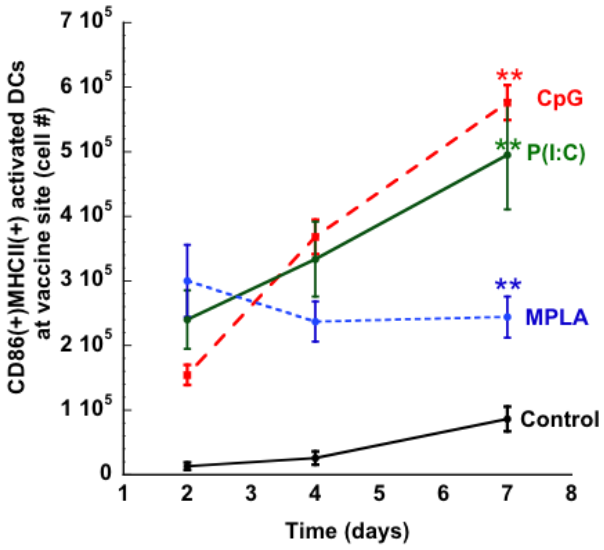

Figure S2 – The kinetics of activated dendritic cell generation at vaccine site. The number of CD86(+)MHCII(+)CD11c(+) dendritic cells present at the vaccine site at 2, 4, and 7 days after implantation of FITC-loaded matrices incorporating, GM-CSF (Control) and matrices loaded with GM-CSF in combination with CpG-ODN (CpG), MPLA (MPLA), and P(I:C) (P(IC)). Values represent mean and standard deviations (n=5). ** $P<0.01$, as compared to control.

Figure S3

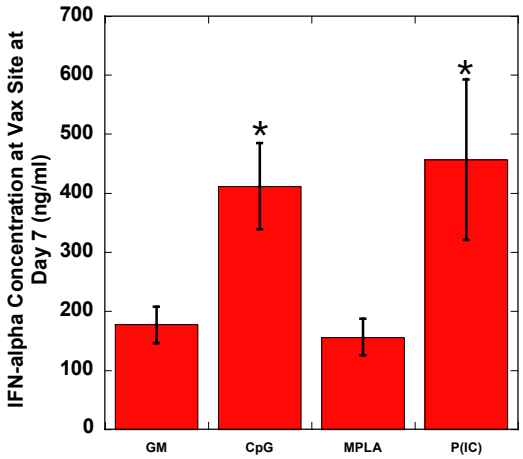

Figure S3 –IFN-α production at vaccine sites. The local IFN-α concentration after implantation of GM-CSF loaded scaffolds (Con) and scaffolds loaded with GM-CSF in combination with CpG-ODN (CpG), MPLA (MPLA), and P(I:C) (P(IC)). Values represent mean and standard deviations (n=5). ** $P<0.01$, as compared to GM-CSF loaded matrices (Con).

Figure S4

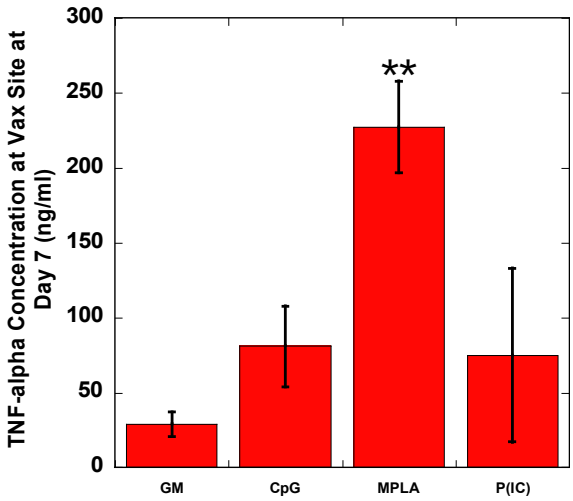

Figure S4 –TNF-α production at vaccine sites. The local TNF-α concentration after implantation of GM-CSF loaded scaffolds (Con) and scaffolds loaded with GM-CSF in combination with CpG-ODN (CpG), MPLA (MPLA), and P(I:C) (P(IC)). Values represent mean and standard deviations (n=5). ** $P<0.01$, as compared to GM-CSF loaded matrices (Con).

Figure S5

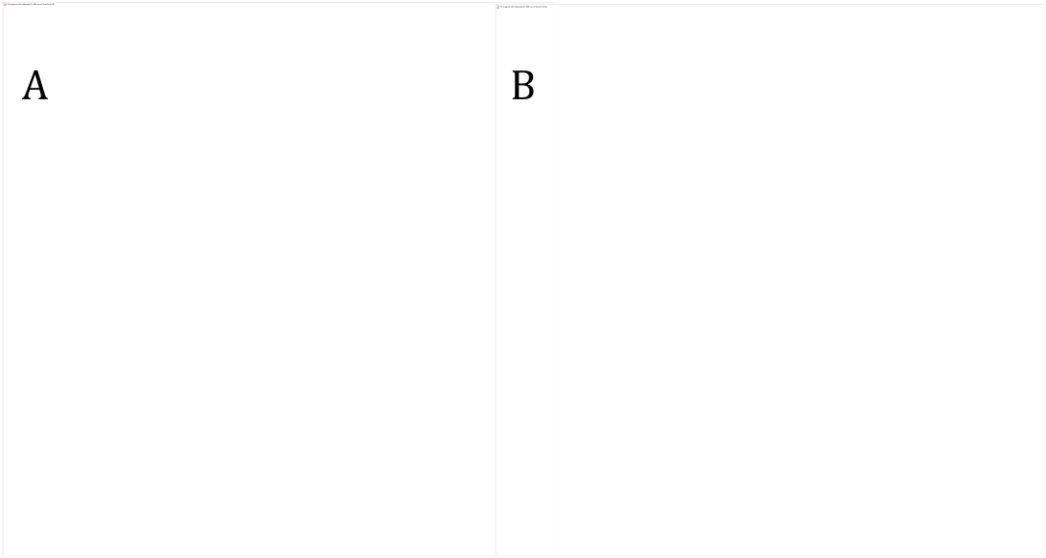

Figure S5 – Prophylactic B16-F10 vaccination in MyD88 and TRIF KO models. (A) MyD88 and (B) TRIF knockout mice were vaccinated with PLG vaccines 14 days prior to B16-F10 melanoma tumor challenge (10^5 cells). (A) A comparison of survival in untreated mice (Control) and mice treated with PLG vaccines loaded with GM-CSF in combination with CpG-ODN (CpG), P(I:C), or MPLA. (n=5)

Figure S6

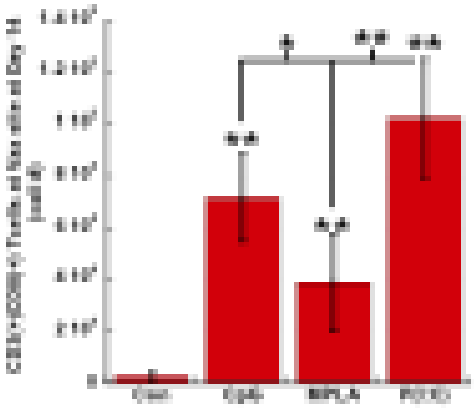

Figure S6 – Vaccine induced T cell recruitment. The total number of CD3(+)CD8(+) T cells isolated from GM-CSF loaded scaffolds (Con) and scaffolds loaded with GM-CSF in combination with CpG-ODN (CpG), MPLA (MPLA), and P(I:C) (P(IC)). Matrices were excised at Day 14 after implantation. Values represent mean and standard deviations (n=5). * $P<0.05$** $P<0.01$, as compared to GM-CSF loaded matrices (Con).

Figure S7

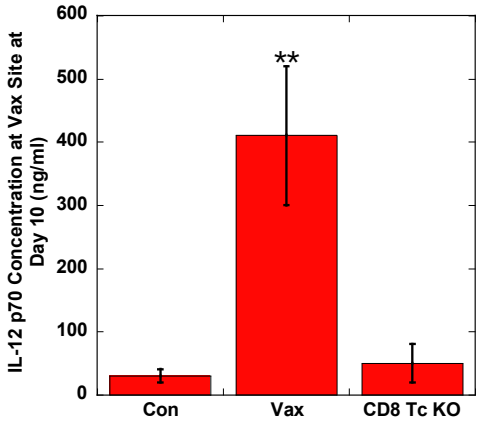

Figure S7 – Comparison of IL-12 production at vaccine sites in wild type and cytotoxic T cell knockout mice. The local IL-12p70 concentration after implantation of GM-CSF loaded scaffolds (Con) and vaccine scaffolds (loaded with tumor lysate, GM-CSF and CpG-ODN) (CpG), in wild type (vax) and B6.129S2-Cd8atm1Mak/J mice (CD8 T cell KO; deficient in cytotoxic T cell activity). Matrices were excised at Day 10 after implantation. Values represent mean and standard deviations (n=5). ** $P<0.01$, as compared to GM-CSF loaded matrices (Con).

Figure S8

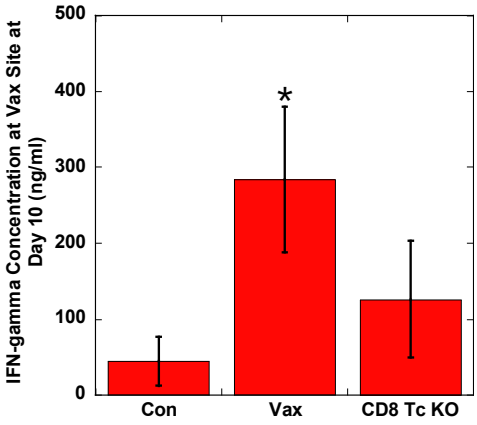

Figure S8 - Comparison of IFN-γ production at vaccine sites in wild type and cytotoxic T cell knockout mice. The local IFN-γ concentration after implantation of GM-CSF loaded scaffolds (Con) and vaccine scaffolds (loaded with tumor lysate, GM-CSF and CpG-ODN)(CpG), in wild type (vax) and B6.129S2-Cd8atm1Mak/J mice (CD8 T cell KO; deficient in cytotoxic T cell activity). Matrices were excised at Day 10 after implantation. *P<0.01, as compared to GM-CSF loaded matrices (Con).

Figure S9

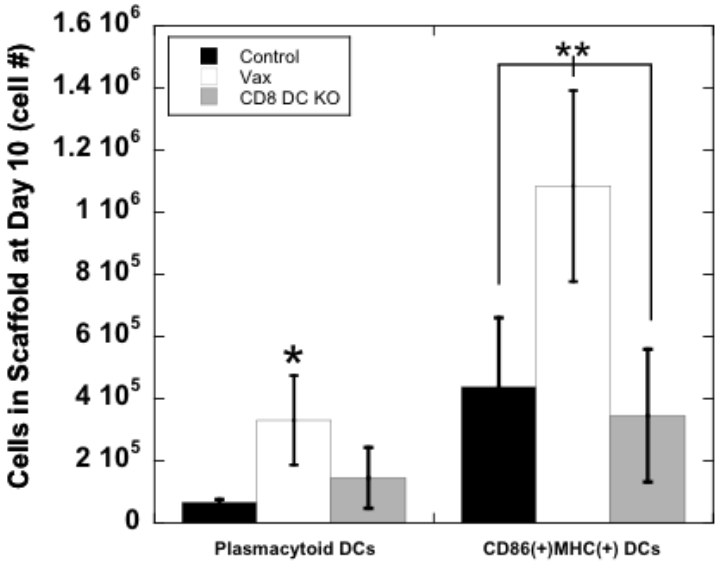

Figure S9 - Comparison of dendritic cell generation at vaccine sites in wild type and CD8 dendritic cell knockout mice. A) The total numbers of plasmacytoid DCs and of activated DCs positive for MHCII and CD86 expression, at the scaffold site at day 10 after implantation of control (Control) and vaccine (Vax) scaffolds in wild type C57BL6/J mice and vaccine scaffolds in Batf3-/- mice (CD8 DC KO). Data represent mean and standard deviation, (n=5). * $P<0.05$, as compared to control matrices unless otherwise noted.

Figure S10

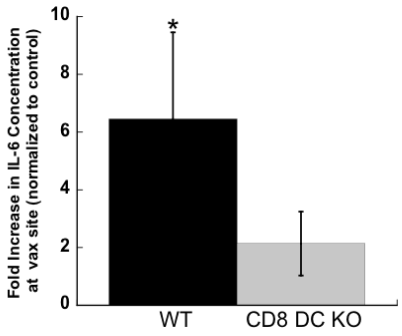

Figure S10 - Comparison of IL-6 production at the vaccine site in wild type and CD8 dendritic cell knockouts. Fold increase in IL-6 concentration at vaccine site of WT and CD8 DC KO mice relative to control matrices. CpG-ODN was the adjuvant utilized in vaccines. Data represent mean and standard deviation, (n=5)* $P<0.05$ ** $P<0.01$.

Figure S11

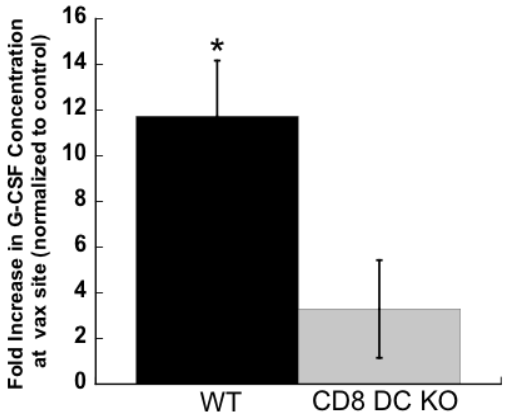

Figure S11 - Comparison of G-CSF production at the vaccine site in wild type and CD8 dendritic cell knockout mice. Fold increase in G-CSF concentration at vaccine site of WT and CD8 DC KO mice relative to control matrices. CpG-ODN was the adjuvant utilized in vaccines. Data represent mean and standard deviation, (n=5)* $P<0.05$ ** $P<0.01$.